Gradation design of porous asphalt mixture (PAM) for low-strength application in wet environment

M. J. Chen and Y. D. Wong

ABSTRACT

Porous asphalt mixture (PAM) is potentially suitable for application in wet environment given its excellent performance in drainage due to the typical open-graded design, whilst ravelling and clogging are the two major issues directly related to the functional service life of PAM pavements. With the increasing up-build of non-motorised transport facility in Singapore which is a tropical country with frequent thunderstorms during monsoon periods, it deserves research into designing well-performing PAM for low-strength pavements such as pedestrian and cycling pathways. In this research, two areas are researched on designing appropriate PAM: firstly, relationship between gradation design and permeability performance is established and 7% content of fine aggregates is selected to achieve adequate coefficient of permeability for Singapore; secondly, four aggregate gradations with different packing structures created by the coarse aggregates were designed, and the performance was evaluated in the aspect of permeability, mechanical strength, resistance to ravelling and resistance to clogging. Three testing scenarios were applied in ravelling and clogging tests, which were unconditioned, ageing-conditioned and moisture-conditioned. It is found that moisture exposure is a more severe condition than ageing on PAM's performance. On the whole, PAM with high content of intermediate size aggregates (i.e. 6.3–4.75 mm) in the coarse fraction and low content (i.e. lower than 7%) of fine fraction is suggested for low-strength PAM pavement in Singapore.

Key works: porous asphalt mixture, packing structure, ravelling test, clogging test, low-strength pavement

1. Introduction

Porous asphalt mixture (PAM) is a typical kind of pervious mixture that possesses extremely high air voids content (usually greater than 20%) as compared with conventional dense asphalt mixtures. Though PAM is not as strong as dense mixtures, PAM's characteristic packing structure engenders excellent drainage, environment and driving benefits, such as reducing aquaplaning, alleviating splash and spray, enhancing skid resistance between pavement and tyres, mitigating traffic noise and generating cooling effect. (Khalid and Jimenez 1995, Nicholls 1997, Fabb 1998, Bruce 2005, Barrett and Shaw 2007, Rungruangvirojn and Kanitpong 2010, Starke et al. 2010). However, ravelling and clogging are the two most critical drawbacks in PAM's performance (Coleri et al. 2013). Ravelling refers to finer particles being stripped from pavement surface due to degraded adhesiveness in the asphalt mastic, and clogging is related to the interconnected air voids within PAM being blocked by dust and/or debris, thereby leading to impaired drainage. Given the distinctive advantages of PAM, it is potentially suitable for paving projects in Singapore, a tropical country encountering high temperature all year around with frequent thunderstorms during the two monsoon periods (Fong 2012). Furthermore, there is an increasing trend in developing non-motorised traffic facility in Singapore, such as pedestrian and cycling pathways (Koh and Wong 2012), and hence there are large requirements in building low-strength pavements. Design of well-performing PAM for specific application, namely low-strength application in the tropical area, is timely and worthy of intensive research.

The distinctive trait of high air voids content in PAM is directly attributed to the open-graded design. Namely, the main aggregate framework is the stone-on-stone interlocking created by coarse aggregates, and the amount of fine aggregates is strictly limited, such as lower than 15–20% (Rajib et al. 2000), therefore, the air voids generated among coarse aggregates are lesser filled in by the fine fraction and asphalt mastic (the composite of asphalt binder and fillers). Hence, proper aggregate gradation design to ensure adequate air voids content which engenders quality drainage performance is important in the PAM design (Roque et al. 1997, Suresha et al. 2009, Mansour and Putman, 2013).

Most aggregate gradation designs and prevailing packing theories are essentially based

on dense asphalt mixtures, such as maximum density curve method and Bailey method (Fuller and Thompson 1907, Good and Lufsey 1965, Vavrik et al. 2002). As for open-graded design, an early work by Furnas (1931) used a binary mixture model which entailed adding proper amount of fine fraction into the coarse aggregate blend to obtain target air voids content, whilst minimum porosity was retained in compacted coarse aggregates through stepwise proportioning (Al-Jarallah and Tons 1981, Hardiman 2004). Zhu (2005) modified Bailey method to achieve target air voids content in PAMs through introducing a volumetric parameter in the asphalt mixture design, namely reserved porosity. Kandhal (2002) developed the voids in coarse aggregate (VCA) method to discern whether a designed PAM possessed sufficient stone-on-stone interlocking; the aggregate framework could be regarded as stable if the ratio of two types of reference VCA indices, namely voids in coarse aggregates of compacted aggregate mixture (VCA_{mix}) and voids in coarse aggregates of coarse aggregate mixture under dry-rodded condition (VCA_{DRC}), was less than 1.0. It can be inferred that air voids content is a critical parameter in PAM gradation design and it is practically achieved by means of appropriately proportioning coarse and fine fractions. On the other hand, little attention has been devoted to researching into the interlocking structure created by coarse aggregates that plays the major role in terms of providing the structural integrity in carrying traffic loads and resisting external deformation.

In current applications, most PAM designs are aimed at motor vehicle roads, such as expressways, arterial roads and collector roads, and principal attention is focused on providing adequate strength to withstand designed traffic volume. However, PAM's performance in resisting ravelling and clogging, which is heavily related to the functional service life, currently receives much less attention in the PAM design. In reality, PAM's functional properties, such as permeability and ravelling resistance, rather than mixture strength, should deserve greater consideration, particularly in the cases of low-strength application, such as pedestrian and cycling pathways, and parking lots.

2. Research objective

The objective of this research was to design appropriate PAM for low-strength application in Singapore, and two main components are involved:

(a) To conduct research on the relationship between aggregate gradation and drainage performance and subsequently to design suitable PAMs that can potentially achieve target permeability;

(b) To conduct a series of performance testing, including conventional and newly designed methods, on the designed PAMs, which possess various interlocking structures created by the coarse aggregates, and subsequently to analyse the suitability of the designed PAMs.

Recommendations for PAM design in the specific application, namely pedestrian and cycling pathways in Singapore, are consequently presented.

3. Research on the relationship between aggregate gradation and drainage performance

Air voids content is a critical factor in PAM design, which is directly related to the essential drainage performance. The high air voids content is basically attributed to the distinctive open-graded design for PAM, namely the amount of fine fraction is much lower than that in the dense asphalt mixture. Herein, a series of aggregate gradations were designed and relevant measurements were carried out, namely volumetric measurements and permeability tests. Target air voids content is usually specified in the design standards to obtain quality performance. For example, a minimum air voids content of 18% is suggested by ASTM (2008). However, in this research, the proper amounts of air voids in a PAM and related fine fraction in the aggregate gradation were assessed based on the relationship between aggregate gradation and permeability in consideration of the permeability requirement for Singapore.

3.1. Materials selection and compaction method

Mineral aggregates and asphalt binder are the two major components in an asphalt mixture. Granite aggregates were applied in this study, and the measured properties are given in Tables 1 and 2. PAM's mixture strength is weaker than conventional dense asphalt mixture due to the low content of fine aggregates, and the resultant high content of air voids exacerbate the moisture and ageing damage. Thus, modified asphalt is widely recommended for PAM design due to the effects in improving ravelling

resistance, rutting resistance, moisture susceptibility, etc. (Rajib et al. 2000, Tayfur et al. 2007, Hsu et al. 2011). PG76 asphalt, which is modified by a type of polymer additive, styrene butadiene styrene (SBS), was applied, with the properties given in Table 3. According to the complex shear modulus elastic portion (G*/sinδ) after rolling thin film oven (RTFO) conditioning, PG76 asphalt is suitable to be applied in area that experiences high temperature like Singapore. Gyration compaction machine was used to fabricate PAM samples as it can better simulate the compaction process in-field as compared to conventional Marshall hammer, and 50 gyrations were selected as a reference gyration count according to AI (1996). Each test was conducted on three replicated specimens.

[Table 1 near here]

[Table 2 near here]

[Table 3 near here]

3.2. Preliminary PAM aggregate gradation design

PAM gradation designs were first reviewed as drawn from various countries and corresponding authorities (Ruiz et al. 1990, JHPC 1994, Rajib et al. 2000, Drainasphaltschichten 2001, AAPA 2004, TNZ 2007, LTA 2010). Based on the uniform design method, which is derived from the theories of ‘number-theoretical method’ and ‘quasi Monte-Carlo method’ (Fang and Ma 2001), eight representative PAM aggregate gradations were designed (see Table 4), denoted as G1–G8 and ordered by the passing percentage on 2.36-mm sieve and 4.75-mm sieve. It can be seen that 5% fillers (namely particles finer than 0.075 mm) were used in all eight aggregate gradations, and there is no fine aggregate of 2.36–0.075 mm in G1 and G2 groups.

Asphalt binder content (ABC) was determined by AI method (AI 1997). Namely, it is based on the estimated surface area (SA) of aggregates in a blend (m2/kg) and the thickness of asphalt film (t). SA can be obtained through Equation (1), and t was selected as 10 μm. The resultant ABC value for each aggregate gradation is shown in Table 4 as well.

$$SA = 0.41 + 0.41a + 0.82b + 1.64c + 2.87d + 6.14e + 12.29f + 32.77g \quad (1)$$

Here, a, b, c ~ g are the percentages by mass of aggregates passing 4.75, 2.36, 1.18, 0.6, 0.3, 0.15 and 0.075-mm sieves, respectively.

[Table 4 near here]

3.3. Measurements for volumetric properties and permeability

Air voids content, including total air voids (TAV) content and water accessible air voids (WAAV) content, are important volumetric parameters for a PAM. TAV content is calculated based on bulk specific gravity (G_{mb}) of the compacted PAM sample and the theoretical maximum specific gravity (G_{mm}) through Equation (2). G_{mb} was determined via the volumetric measurement and G_{mm} was measured via a vacuum pycnometer.

$$TAV = \left(1 - \frac{G_{mb}}{G_{mm}}\right) \times 100 \quad (2)$$

WAAV content was measured via buoyancy principle and calculated through Equations (3) and (4).

$$WAAV = \frac{V_{WAAV}}{V} \times 100 \quad (3)$$

Here, V_{WAAV} is the volume of inter-connective air voids, which can be obtained through Equation (4), and V is the volume of PAM, which was measured through dimensional method.

$$V_{WAAV} = V - (V_m + V_{WIAV}) = V - \frac{W_{air} - W_{water}}{\gamma_w} \quad (4)$$

Here, V_m is the volume of the materials (namely aggregates covered with asphalt binder) in the compacted sample, V_{WIAV} is the volume of the WAAV, W_{air} is the weight of compacted sample in air, and W_{water} is the weight of compacted sample immersed in water (recorded when the reading on the weighing scale has stabilised), and γ_w is unit

density of water.

Permeability is the essential function of PAM, which directly improves driving safety, such as reducing aquaplaning and alleviating splash and spray. Permeability testing apparatus as developed by Florida DOT (2004) was used in this research, and the coefficient of permeability, *k*, can be obtained through Equation (5).

$$k = \left(\frac{aL}{At}\right) \times \ln\frac{h_1}{h_2} \times t_c \tag{5}$$

Here, *a* is the internal cross-sectional area of burette (cm^2), *L* is the mean thickness of PAM sample (*cm*), *A* is the cross-sectional area of PAM sample (*cm2*), h_1 and h_2 are the initial and final water heads across PAM sample (*cm*), *t* is elapsed time for water passing from h_1 to h_2 (*s*) and t_c is temperature correction coefficient. The measured permeability is partially influenced by the water head (Ranieri et al. 2012, Ranieri, Ying et al. 2012). Florida permeameter used in this research is a falling-head permeameter. The initial water head, h_1, equals to h_2 + *62.4* cm; the final hydraulic head, h_2, equals to *L + 26.6 cm*.

3.4. Analysis of results

For each of the eight PAM designs, three replicated samples were fabricated, and the volumetric parameters of each sample were measured before determination of permeability. The breaking sieve (BS), which distinguishes the coarse and fine fractions in an aggregate blend, is conventionally selected as 4.75 mm for asphalt mixture design. Though various packing theories have been developed and the related sizes of BS have been re-examined (Vavrik et al. 2002, Watson et al. 2004), the resultant BS usually turned out to be 2.36 mm or 4.75 mm. Based on the relationship between air voids content (TAV and WAAV contents) and the content of aggregates passing 2.36 and 4.75 mm among the eight designed PAMs (see Figures 1 and 2), it can been seen that there is a strong correlation between air voids content (i.e. TAV or WAAV content) and passing 2.36-mm aggregate content. It should be noted that, for each of the eight PAM designs, gradation curve below 2.36 mm is relatively smoother than that above 2.36 mm which possesses more variations, and the assigned ABC is related to gradation design. This

might strengthen the correlation between air voids content and passing 2.36-mm aggregate content. On the other hand, an erratic correlation is observed in the contents between air voids and aggregates passing 4.75 mm. Hereby, content of aggregates finer than 2.36 mm provides a better relationship with the air voids content generated in the PAM samples. In other words, aggregates passing 2.36-mm sieve can play a more consistent role of filling voids than that passing 4.75-mm sieve, hence it is more suitable to regard 2.36-mm sieve as the BS for PAMs.

[Figure 1 near here]

[Figure 2 near here]

With respect to drainage performance, PAM's permeability performance is generally enhanced with the increase in air voids content (TAV or WAAV content). The correlation profiles (power curves), namely (a) curve of TAV content and *k* value (i.e. coefficient of permeability) and (b) curve of WAAV content and *k* value, are almost parallel, especially for *k* values larger than 50×10^{-3} cm/s (see Figure 3), while noting the linear relationship between TAV and WAAV contents (see Figure 4).

[Figure 3 near here]

[Figure 4 near here]

According to the practical amount of precipitation in Singapore, peak rainfall can reach 130×10^{-3} cm/s during monsoon period (NEA 2014). Hence, the required coefficient of permeability was selected as 130×10^{-3} cm/s in this research, instead of suggested value by ASTM (2008), namely permeability/porosity value higher than 115.7×10^{-3} cm/s. Based on the relationship between permeability and TAV content (see Equation (6)), PAM's permeability can meet the requirement (namely $k \geqslant 130 \times 10^{-3}$ cm/s) when TAV is no lower than 22.3%. Subsequently, the content of passing 2.36-mm aggregates was selected as 7% according to the relationship with TAV content, as given in Equation (7).

$$y = 3E - 05x^{4.9253} \ (R^2 = 0.925) \tag{6}$$

Here, y denotes coefficient of permeability (k, $\times 10^{-3}$ cm/s), and x denotes TAV content.

$$y' = -0.8504x' + 28.244 \ (R^2 = 0.948) \tag{7}$$

Here, y' denotes the TAV content, and x' denotes the aggregate content passing 2.36 mm.

4. Designing aggregate gradations for low-strength application

Aggregate interlocking is an important factor to an asphalt mixture's capability in resisting external loading. In the case of PAM, in which the content of fine fraction is relatively lower as compared to conventional dense asphalt mixture so as to achieve high air voids content, the aggregate interlocking created by coarse aggregates will be directly related to PAM's property. Herein, several PAMs with different interlocking structures created by coarse aggregates were designed, and the resultant properties were measured and evaluated. Especially, PAM's performance in resisting ravelling and clogging, namely the two main issues associated with PAM, were evaluated via conventional and newly designed testing methods.

4.1. PAM design for specific application

According to the results in Section 3.4, the content of fine fraction was selected as 7% for potential PAMs to achieve adequate permeability, and four PAMs with different structures in coarse aggregates were designed (see Table 5 and Figure 5), as follows:

(a) G_cont: the coarse fraction was relatively continuously distributed, namely the shape of the coarse fraction was similar to Fuller's curve;

(b) G_coarse: the content of large-size aggregates was very high, such that the content of aggregates retained on 9.5 and 6.3 mm were 55 and 80%, respectively;

(c) G_fine: the content of small-size aggregates in coarse fraction, namely 4.75–2.36 mm, was high, which equalled to 38%; and

(d) G_S: the curve of the coarse fraction was 'S-shape', namely the aggregates with intermediate size (i.e. 6.3–4.75 mm) was high, which equalled to 40% (see Figure 5).

The content of fillers was kept as 5%, and particles with size of 2.36–0.075 mm were uniformly distributed. The ABC was selected as 4% by mixture weight for all the four PAMs. Since aggregate surface area in a blend is mainly dependent of the amount of fine aggregates, the thicknesses of asphalt binder in the four PAM designs were similar (e.g. 11.3 ± 0.16 μm) given the same content of asphalt binder (i.e. 4%) and the same content of passing 2.36-mm aggregates (i.e. 7%) according to AI (1997). Though the selected ABC is relatively low, it is potentially feasible considering the lower requirement in mixture strength for low-strength application (AAPA 2002).

[Table 5 near here]

[Figure 5 near here]

4.2. Performance evaluation

4.2.1. Volumetric properties and permeability

For each performance test, three replicate specimens for each gradation design were prepared, and air voids content (namely TAV and WAAV contents) and permeability were measured before testing except the ones for Cantabro abrasion tests. WAAV ratio, namely the proportion of WAAV in TAV content (see Equation (8)), was determined as well.

$$WAAV\ ratio = \frac{WAAV\ content}{TAV\ content} \times 100\% \tag{8}$$

4.2.2. Draindown test

Draindown refers to asphalt mastic flowing downwards within an asphalt mixture. It tends to occur in high-temperature environment, such as during mixing and compacting process, especially in the cases of high ABC. In the laboratory, draindown test is carried on loose asphalt mixture sample at assigned ABC. The sample is poured into a wire basket (2.36-mm mesh size) with a catch tray below and heated in an oven at mixing temperature. The asphalt mastic drains into the tray after one hour heating is recorded, and the corresponding mass loss by percentage is regarded as draindown value. According to Rajib et al. (2000), draindown value should not be higher than 0.3% by

mass.

4.2.3. Mechanical strength

Marshall test is a conventional method in assessing an asphalt mixture's mechanical strength. The specimen undergoes a vertical load at a constant speed of 50.8 mm/min until failure, and the peak load that can be carried is recorded as Marshall stability (MS). Two kinds of Marshall test were conducted in this research to assess the strength of PAMs, namely (a) unconditioned Marshall test: the specimen was conditioned in a water bath at 60 °C for 30 min before loading; and (b) moisture-conditioned Marshall test: the specimen was conditioned in a water bath at 60 °C for 24 h before loading (STP 1993). The testing results are given as unconditioned Marshall stability (UC-MS) and moisture-conditioned Marshall stability (MC-MS), respectively, and retained Marshall stability was calculated using Equation (9).

$$retained\ MS = \frac{\text{MC-MS}}{\text{UC-MS}} \times 100\% \tag{9}$$

Marshall test is a standard mechanical strength test in Singapore, and the required lower limit of UC-MS is 9.0 kN for normal application (LTA 2010). However, in the case of low-strength application, the requirement can be lowered to 4.0 kN (AAPA 2002).

Indirect tensile stiffness modulus (ITSM) test was conducted in two scenarios as well, namely unconditioned and moisture-conditioned. Material testing apparatus was utilised to apply a compression load in the vertical diametric plane of PAM sample with a haversine loading wave shape, and the relative testing parameters are given in Table 6 (AS 1995). Testing results are given as unconditioned ITSM (UC-ITSM) and moisture-conditioned ITSM (MC-ITSM), respectively, and retained ITSM was determined using Equation (10). Additionally, given that ITSM test is non-destructive, the specimen used in unconditioned test was subsequently applied in moisture-conditioned test.

$$retained\ \text{ITSM} = \frac{\text{MC-ITSM}}{\text{UC-ITSM}} \times 100\% \tag{10}$$

[Table 6 near here]

4.2.4. Cantabro abrasion test

Cantabro abrasion test is a conventional method to assess PAM's performance in resisting ravelling. To simulate the effect of ravelling, the specimen undergoes 300 revolutions in a Los Angeles (LA) machine at 25 ± 5 °C at a speed of 30–33 rpm, and the abrasion loss value (ALV) is represented as the mass loss during abrasion in per cent, as shown in Equation (11).

$$ALV = \left(\frac{P_1 - P_2}{P_1}\right) \times 100 \tag{11}$$

Here, P_1 and P_2 are the initial and finial masses of the specimen, respectively.

Cantabro abrasion test in three testing scenarios were carried out in this research: (a) unconditioned: test was conducted as specimen was cooled down to room temperature (i.e. 25 °C) after fabrication; (b) ageing-conditioned: specimen was conditioned in an oven at 60 ± 1 °C for seven days and cooled down later before testing (ASTM 2008); and (c) moisture-conditioned: specimen was conditioned in a water bath at 60 ± 1 °C for 1 day and subsequently was put in a ventilated room for one day so as to evaporate most of the moisture retained in the specimen before testing. The testing results are represented as unconditioned abrasion loss value (UC-ALV), ageing-conditioned abrasion loss value (AC-ALV) and moisture-conditioned abrasion loss value (MC-ALV), respectively. The suggested upper limits of UC-ALV, AC-ALV and MC-ALV are 20, 30 and 35%, respectively (Rajib et al. 2000, Alvarez et al. 2010).

In addition, given that most abrasion effect involved in Cantabro abrasion test is the impact between specimen and drum wall of the LA machine, which is overly severe as compared with the practical abrasion effect on pavement surface, a reduced abrasion effect has been suggested (Dong et al. 2013). In this research, ALV values were recorded at intervals of 50 revolution counts.

4.2.5. Clogging resistance test

Clogging is another critical problem with PAM, referring to the deterioration in permeability due to dust and/or debris blocking the air voids in PAM. Clogging is related to the initial permeability and size-based granulometric index as well (Ranieri et al. 2010). However, there is no widely accepted test which has been approved for evaluating PAM's performance in resisting clogging. Based on previous research work (Fwa et al. 1999, Tan et al. 2000), a process of clogging/de-clogging was designed, and the effect on PAM's permeability was measured so as to evaluate PAM's performance in resisting clogging.

Two batches of granite dust with different size distributions were applied as clogging material (CM), namely CM1 and CM2, possessing the maximum particle size of 600 and 300 μm, respectively (see Figure 6).

[Figure 6 near here]

The testing procedure is as follows:

(1) place PAM specimen in the permeability testing apparatus

(2) clogging/de-clogging cycle

(i) clogging process: scatter 5 grams CM on the specimen surface uniformly and subsequently apply 100 *ml* of water to make CM penetrate into the specimen, and permeability is measured after clogging;

(ii) de-clogging process: apply 2000 *ml* of water through the specimen as a de-clogging process and measure the permeability meanwhile, and repeat the de-clogging process five times to record the permeability recovery;

(3) repeat clogging/de-clogging cycle five times.

Three testing scenarios were involved in clogging resistance tests as well, namely unconditioned, ageing-conditioned and moisture-conditioned, and the conditioning methods for ageing and moisture cases were the same as that in previous tests. Retained permeability (i.e. retained k value) was calculated along the process of clogging/de-clogging process through Equation (12).

$$retained\ k = \frac{k_1}{k_2} \times 100\% \tag{12}$$

Here, k_1 is the initial coefficient of permeability, namely the one without conditioning or clogging/de-clogging; and k_2 is the coefficient of permeability after conditioning or clogging/de-clogging.

4.3. Results and discussion

4.3.1. Air voids content and permeability

Different values of air voids content and permeability were obtained (see Table 7), which was probably due to the different voids structure based on the aggregate size distribution in the four PAMs. As the coarse fraction contained more large- and/ or intermediate-size stones, namely the cases of G_coarse and G_S, more air voids contents (i.e. TAV and WAAV contents) were generated in these PAMs as compared with the other two PAM designs. Meanwhile, higher WAAV ratios were obtained in G_ coarse and G_S; namely, effective air voids were created at higher ratios among the TAVs, and hereby the resultant coefficients of permeability were higher as well. However, comparing G_coarse and G_S, the one that possessed relatively higher WAAV content and WAAV ratio, namely G_coarse, showed relatively lower permeability. This can be explained that the high content of inter- mediate-size aggregates in G_S generated air voids with sizes that were relatively more uniformly distributed. Consequently, water can flow through the specimen more fluently, as consistent with the findings by Poulikakos and Partl (2010) that PAM with better functionality can be achieved with air voids of more homogeneous structure. Additionally, although the contents of fine fraction in the four PAM designs were the same, namely 7%, only G_coarse and G_S could meet the suggested permeability in Singapore, namely being higher than 130×10^{-3} cm/s.

[Table 7 near here]

4.3.2. Draindown test

For each of the four PAM designs, no obvious drained down asphalt mastic was

observed after the loose asphalt mixture was heated in the oven at mixing temperature for one hour. It is indicated that draindown was not an issue for the four PAM designs, which was attributed partially to the relatively low ABC.

4.3.3. Marshall test

UC-MS values of the four PAM designs can all meet the requirement for low-strength application, namely being greater than 4.0 kN, and the difference in UC-MS among the four PAM designs was relatively slight, with the MS values of G_cont and G_fine being a little higher as compared with the other two designs (see Table 8), which is attributed to the relatively lower air voids content. In the aspect of moisture conditioning, the values of retained MS remained high for most PAM designs, and each design even possessed MC-MS value higher than 4.0 kN, indicating moisture exposure was not a debilitating issue in Marshall test performance.

[Table 8 near here]

4.3.4. ITSM test

Whereas Marshall test estimated the peak load that can be carried by specimen during constant loading, ITSM test measures asphalt mixture's capability in recovering the deformation upon external loading/unloading. It can be seen that G_coarse and G_fine possessed lower UC-ITSM and MC-ITSM values as compared with the other two PAM designs, implying that the resilient behaviour is weaker for high content of large- or small-size aggregates in the coarse fraction (see Table 9). After moisture conditioning, retained ITSM value in G_fine was the lowest among the four designs, with MC-ITSM value in G_S being close to G_cont and G_coarse, which may be ascribed to the higher air voids content.

[Table 9 near here]

4.3.5. Cantabro abrasion test

In all the three testing scenarios, ALV value for each PAM design increased consistently with the revolution count (see Figures 7–9). In the case of unconditioned Cantabro abrasion test, all four PAM designs can meet the 20% requirement in UC-ALV's upper

limit. The PAM design with a high content of small-size aggregates in the coarse fraction, namely G_fine, showed the strongest resistance to Cantabro abrasion among the four designs, and its final UC-ALV value after the total 300 revolutions was lower than 10%, followed by G_S, G_cont and G_coarse. This suggests that stronger resistance to Cantabro abrasion can be achieved with higher content of small- or intermediate-size aggregates in the coarse fraction, while PAM designs with more large-size aggregates, such as G_coarse, showed weaker resistance in maintaining integrity of the specimens during Cantabro abrasion.

[Figure 7 near here]

[Figure 8 near here]

[Figure 9 near here]

Due to the high air voids content in PAM, ageing and oxidation in asphalt binder tended to occur more rapidly as compared to dense asphalt mixture, resulting in larger reduction in the adhesiveness of asphalt mastic and weaker resistance to abrasion (Herrington et al. 2005, Alvarez et al. 2010). In the case of ageing-conditioned Cantabro abrasion test, AC-ALV values in all PAM designs were lower than the 30% upper limit. For G_coarse and G_S, AVL values after ageing conditioning were slightly larger than that in the unconditioned scenario, and the corresponding increases were 6.3 and 13.4%, respectively. For G_cont, the resistance to Cantabro abrasion after ageing condition was well retained as that in unconditioned scenario. On the other hand, AC-ALV value of G_fine was almost 1.9 times higher than its UC-ALV value, indicating ageing conditioning was more severe for PAMs with a high content of small-size aggregates in coarse fraction as compared with the packing structures created in the other three PAM designs. This is probably due to the relatively thinnest asphalt film in G_fine, given that the total surface area of aggregates in G_fine was the largest for the high content of small-size aggregates in the aggregate gradation and the ABC was the same (namely 4%) among the four PAMs. Consequently, adhesiveness in asphalt binder degraded most in G_fine during ageing conditioning and engendered high AC-ALV value, with consistent with the findings by Suresha et al. (2010).

In the case of moisture-conditioned Cantabro abrasion test, the PAM specimens of all the four designs were harshly degraded after 300 revolutions, with MC-ALV values being larger than 70%, indicating that moisture exposure is a serious issue in Cantabro abrasion. The relatively low content of asphalt binder probably contributed to the PAMs' poor performance in moisture-conditioned Cantabro abrasion test. Thus, higher ABC is recommended to strengthen the PAM specimens and meet the recommended requirement of MC-ALV value, namely lower than 35% (Alvarez et al. 2010). On the other hand, MC-ALV at low revolution counts, such as 50, 100 or 150 revolutions, can be applied in assessing PAM's resistance to ravelling, given that the breakage effect of Cantabro abrasion would be much more severe as compared with the practical ravelling effect on the pavement surface. It can been seen that, for all the four PAM designs, MC-ALV values were lower than 20% at 50 revolutions and started to become higher than 40% at 150 revolutions. Meanwhile, along the whole process of Cantabro abrasion, MC-ALV in G_fine was the lowest, followed by G_S, G_cont and G_coarse, which is similar to the case in unconditioned scenario.

On the whole, PAM's resistance to Cantabro abrasion is strongly related to the packing structures created by aggregates. In unconditioned and moisture-conditioned scenarios, PAM specimens with a higher content of small- or intermediate-size aggregates showed stronger resistance during the process of Cantabro abrasion. Meanwhile, PAM's resistance to abrasion was affected by the adhesiveness of asphalt binder as well. In ageing-conditioned scenario, thinner thickness of asphalt film tended to be oxidised more rapidly and resulted in weaker resistance to abrasion, as shown in G_fine design.

4.3.6. Clogging resistance test

Two kinds of clogging material, namely CM1 (<600 μm) and CM2 (<300 μm) were applied to assess PAM's resistance to clogging, namely the capability in retaining permeability, in the unconditioned scenario. It can be seen that permeability decreased upon clogging, and gradually recovered partially during the process of de-clogging, which was simulated via flushing with 2000 ml of water (see Figures 10 and 11). As compared with CM1, permeability tended to be recovered to a higher degree for each PAM design using CM2, given that finer size particles are easier to be flushed out from the PAM specimens.

[Figure 10 near here]

[Figure 11 near here]

Considering that permeability tended to be largely recovered after clogging/de-clogging process with CM2 as clogging material, CM1 with coarser particles was applied to assess PAM's resistance to clogging in the more severe ageing-conditioned and moisture-conditioned scenarios. It can be seen that after ageing-conditioning (without clogging/de-clogging process), retained *k* values all remained very high in the four PAM designs as compared with the retained *k* values after moisture-conditioning, indicating moisture exposure had more severe effect in impairing PAM's drainage capability. However, in each PAM design, the development of *k* value along the process of clogging/de-clogging process was similar to that in unconditioned scenario as shown in Figure 10, resulting in the final *k* values (after five cycles of clogging/de-clogging process) being very similar among all three scenarios (see Table 10). In terms of *k* value after conditioning (i.e. ageing conditioning or moisture conditioning), G_coarse still possessed the highest permeability, followed by G_S, G_fine and G_cont, which is similar to the case in unconditioned scenario. It is indicated that, as compared with PAMs containing more small-size aggregates in coarse fraction, PAMs with higher content of large- and/or intermediate-size aggregates possessed better resistance to clogging, namely a higher permeability is achieved over clogging/de-clogging process, which is probably attributed to the air voids of larger size and at higher content that are generated by the larger aggregates in the PAM specimens. Additionally, it is suggested to regularly remove the dust and/or debris on the surface of or inside the PAM pavements by means of relevant cleaning machines, such as high-pressure jets of water and vacuum suction, so as to maintain acceptable drainage performance especially during monsoon periods.

[Table 10 near here]

5. Conclusions and discussions

This research aims at developing procedures for designing suitable PAM for low-strength application in Singapore, which is realised

through two main components: firstly, establishing the relationship between PAM's aggregate gradation and permeability performance; secondly, four potential PAMs were designed and relevant performance, namely permeability, mechanical strength, ravelling resistance and clogging resistance, was evaluated through laboratory experiments.

5.1. Conclusions

According to the gradation–permeability relationships, it is found that sufficient permeability can be realised with fine fraction (i.e. aggregates finer than 2.36 mm) being lower than 7%. The content of fine fraction was thus selected as 7% and four PAMs encompassing different packing structures created by the coarse aggregates were designed: (a) G_cont, the coarse fraction was generally continuously distributed, (b) G_coarse, content of large-size stones (i.e. 19.0–6.3 mm) in coarse fraction was high, (c) G_fine, content of small-size aggregates (i.e. 4.75–2.36 mm) in coarse fraction was high and (d) G_S, content of intermediate-size aggregates (i.e. 6.3–4.75 mm) in coarse fraction was high.

Experimental results showed that PAM's drainage-related performance, such as permeability and clogging resistance, are greatly influenced by the size and distribution of air voids within the specimens, which is directly related to the packing structure created by the coarse aggregates. Higher air voids content was generated as the content of large- and/or intermediate-size aggregates was higher in open-gradation design, such as G_coarse and G_S, and WAAV ratio was larger meanwhile, namely inter-connected air voids are generated at a higher rate within the TAVs, leading to higher permeability. Moreover, as compared to G_coarse, G_S possessed higher permeability, which was majorly attributed to the more uniformly distributed air voids that were generated by the high content of intermediate-size aggregates. In terms of clogging resistance, G_coarse showed the highest permeability along the clogging/de-clogging process among the four PAM designs in all the testing scenarios (namely unconditioned, ageing-conditioned and moisture-conditioned), which was attributed to the higher content of large-size air voids created by high content of large-size aggregates in coarse fraction.

In the aspect of ravelling resistance, all the four PAM designs can meet the requirements suggested for unconditioned and ageing-conditioned Cantabro abrasion tests. Generally,

PAM designs with higher content of small- and/or intermediate-size aggregates showed stronger in Cantabro abrasion test. On the other hand, large reduction in adhesiveness of asphalt binder after ageing conditioning can heavily weaken PAM's ravelling resistance. Considering that ravelling in Cantabro abrasion test is much more severe than practical ravelling in the field, a lower revolution count is suggested for assessing PAM's resistance abrasion, such as 50, 100 or 150 revolutions, and further research can be conducted in developing new testing method of PAM's ravelling resistance to better simulate practical ravelling on pavement surface. In both ravelling and clogging resistance tests, moisture is a more serious condition for PAM as compared to ageing. Thus, additives to enhance PAM's resistance to moisture-related damage are recommended, such as 2% hydrated limes as fillers.

In terms of mechanical strength, UC-MS values in all the four PAM designs were higher than the lower limit suggested for low-strength application (i.e. 4.0 kN), so were the MS values after moisture conditioning. On the whole, among the four PAM designs, PAMs with higher content of air voids content, namely G_coarse and G_S, generally possessed higher performance in permeability and clogging resistance, while G_S showed stronger resistance to ravelling in the three testing scenarios. Thereby, PAM with fine fraction at 7% and 'S-shape' in the gradation curve of coarse fraction, namely with high content of intermediate-size aggregates, is recommended for the low-strength application in Singapore.

5.2. Discussions

It should be cautioned that pervious pavement's performance in drainage is not only dependent on the PAM's coefficient of permeability alone, but also relates to the road geometric design (e.g. longitudinal slope, cross slope, road width and surface thickness) and drainage facilities underneath and along the roads (Tan et al. 2004, Charbeneau and Barrett, 2008, Ranieri, Ying et al. 2012). Thus, for specific application, this kind of practical conditions should be taken into account to modify the PAM design, especially in selecting the target coefficient of permeability and/or target air voids content.

In addition, PAM's permeability as measured in the laboratory may not correlate well with pavement drainage in the field due to the varying environmental situations,

clogging materials and traffic conditions. In future work, it is desirable to undertake field validation by conducting in-field permeability tests and relevant clogging resistance tests on different types of trial pavement sections. For example, four types of test sites are suggested, denoted as L1–L4: L1, a parking lot with covered shelter; L2, a shared pedestrian-cycling pathway alongside a local access road; L3, a shared pedestrian–cycling pathway alongside an arterial road; and L4, the carriageway of an arterial road. Whereas L1 site has relatively the mildest environment (without exposure to rainfall or severe ageing from direct sunlight, and limited traffic flow), L2, L3 and L4 sites are exposed to progressively more dusts and debris (clogging materials) from the heavier traffic flows, especially the heavy trucks. In this way, the loading effect of the clogging materials can be compared. Evaluation tests are to be conducted for different periods of the year that straddle different rainfall intensity, and hence the de-clogging effect of rainfall intensity is established.

Acknowledgements

The authors would like to thank Shell Bitumen Singapore for supplying PG76 asphalt. The authors also thank the graduating bachelor degree's students in characterising some of the material properties.

References

AAPA, 2002. Light duty asphalt pavement. No. IG-5. Kew Victoria: Australian Asphalt Pavement Association [AAPA].

AAPA, 2004. National asphalt specification. 2nd ed. Kew Victoria: Australian Asphalt Pavement Association [AAPA].

AI, 1996. Superpave design method. Lexington, KY: Asphalt Institute [AI].

AI, 1997. Mix design methods for asphalt concrete and other hot-mix types. Lexington, KY: Asphalt Institute [AI].

Al-Jarallah, M. and Tons, E., 1981. Void content prediction in two-size aggregate mixes. Journal of Testing and Evaluation, 9 (1), 1–10.

Alvarez, A.E., et al., 2010. Evaluation of durability tests for permeable friction course mixtures. International Journal of Pavement Engineering, 11 (1), 49–60.

AS, 1995. Method 13.1: Determination of the resilient modulus of asphalt- indirect tensile method. AS 2891.13.1. Australian Standard [AS].

ASTM, 2008. Standard practice for open-graded friction course (OGFC) mix design. Vol. D7064-08. Philadephia, PA: American Society for Testing and Materials [ASTM].

Barrett, M.E. and Shaw, C.B., 2007. Benefits of porous asphalt overlay on storm water quality. Transportation Research Record: Journal of the Transportation Research Board, 2025, 127–134.

Bruce, K.F., 2005. Porous pavements. Boca Raton, FL: Taylor & Francis.

Charbeneau, R.J. and Barrett, M.E., 2008. Drainage hydraulics of permeable friction courses. Water Resources Research, 44 (4).

Chen, M.J. and Wong, Y.D., 2016. Evaluation of the development of aggregate packing in porous asphalt mixture using discrete element method simulation. Road Materials and Pavement Design. Available from: http://www.tandfonline.com/doi/abs/10.1080/14680629.2016.1138881?journalCode=trmp20

Coleri, E., et al., 2013. Clogging evaluation of open graded friction course pavements tested under rainfall and heavy vehicle simulators. Journal of Environmental Management, 129, 164–172.

Dong, Q., et al., 2013. Investigation into laboratory abrasion test methods for pervious concrete. Journal of Materials in Civil Engineering, 25 (7), 886–892.

Drainasphaltschichten, 2001. Standards for porous asphalt. SN 640 433b, Konzeption Anforderung, Ausführung.

Fabb, T.R.J., 1998. Porous asphalt surface courses. In: J.C. Nicholls, ed. Asphalt surfacings. London: Spon Press, 187–218.

Fang, K.T. and Ma, C.X., 2001. Orthogonal and uniform experimental design (in Chinese). Beijing: Science Press.

Florida DOT, 2004. Florida method of test for measurement of water permeability of compacted asphalt paving mixture. FM5-565. FL: Department of Transportation.

Fong, M., 2012. The weather and climate of Singapore. Singapore: Meteorological Service Singapore.

Fuller, W.B. and Thompson, S.E., 1907. The Laws of proportioning concrete. Journal of Transportation Division, 59, 67–143.

Furnas, C.C., 1931. Grading aggregates I-mathematical relations for beds of broken solids of maximum density. U.S. Bureau of Mines, 23 (9), 1052–1058.

Fwa, T.F., Tan, S.A. and Guwe, Y.K., 1999. Laboratory evaluation of clogging potential of porous asphalt mixtures. Transportation Research Record: Journal of the Transportation Research Board, 1681, 43–49.

Good, J.F. and Lufsy, L.A., 1965. Voids, permeability, film thickness vs. asphalt hardening. Proceedings, Association of Asphalt Pavement Technologists [AAPT], vol. 34.

Hardiman, H., 2004. Application of packing theory on grading design for porous asphalt mixtures. Civil Engineering Dimension, 6 (2), 57–63.

Herrington, P.R., Reilly, S. and Cook, S., 2005. Porous asphalt durability test transfund New Zealand research report. No. 265. Lower Hutt: Opus International Consultants, Central Laboratories.

Hsu, T.W., Chen, S.C. and Hung, K.N., 2011. Performance evaluation of asphalt rubber in porous asphalt-concrete mixtures. Journal of Materials in Civil Engineering, 23 (3), 342–349.

JHPC, 1994. Design and execution manual for porous asphalt. Haisuisei- hosou Sekkei Sekou Manual. Tokyo: Japan Highway Public Corporation [JHPC].

Khalid, H. and Jimenez, P.F.K., 1995. Performance assessment of Spanish and British porous asphalts performance and durability of bituminous materials. London: Spon Press.

Kandhal, P., 2002. Design, construction, and maintenance of open-graded asphalt friction courses. Information series 115, Lanhuam, MD: National Asphalt Pavement Association [NAPA].

Koh, P.P. and Wong, Y.D., 2012. The evolution of cycling in Singapore. Journeys, 9, 39–50.

LTA, 2010. Engineering group materials & workmanship specification for civil & structural works. Singapore: Land Transport Authority.

Mansour, T.N. and Putman, B.J., 2013. Influence of aggregate gradation on the performance properties of porous asphalt mixtures. Journal of Materials in Civil Engineering, 25 (2), 281–288.

NEA, 2014. Weatherwise Singapore. [Online]. Singapore: National Environment Agency [NEC]. Available from: http://app2.nea.gov.sg/weather-climate/climate-information/weather-statistics [Accessed 27 July 2014].

Nicholls, J.C., 1997. Review of UK porous asphalt trials. Vol. TRL Report 264. London: Transport Research Laboratory [TRL].

Poulikakos, L.D. and Partl, M.N., 2010. Investigation of porous asphalt microstructure using optical and electron microscopy. Journal of Microscopy, 240, 145–154.

Rajib, B.M., Prithvi, S.K., Cooley, L.A. and Donald, E.W., 2000. Design, construction, and performance of new-generation open-graded friction courses. Auburn, AL: National Center for Asphalt Technology [NCAT].

Ranieri, V., Sansalone, J.J. and Shuler, S., 2010. Relationships among gradation curve, clogging resistance, and pore-based indices of porous asphalt mixes. Road Materials and Pavement Design, 11, 507–525.

Ranieri, V., et al., 2012. Measurement of hydraulic conductivity in porous mixes. Transportation Research Record: Journal of the Transportation Research Board, 2295, 1–10.

Ranieri, V., Ying, G. and Sansalone, J., 2012. Drainage modeling of roadway systems with porous friction courses. Journal of Transportation Engineering, 138 (4), 395–405.

Roque, R., Huang, S. and Ruth, B.E., 1997. Maximizing shear resistance of asphalt mixtures by proper selection of aggregate gradation. The 8th International Society for Asphalt Pavements, Seattle, WA, 249–268.

Ruiz, A., et al., 1990. Porous asphalt mixtures in Spain. Transportation Research Record, 1265, 87–94.

Rungruangvirojn, P. and Kanitpong, K., 2010. Measurement of visibility loss due to splash and spray: porous, SMA and conventional asphalt pavements. International Journal of Pavement Engineering, 11 (6), 499–510.

Starke, P., Gobel, P. and Coldewey, W.G., 2010. Urban evaporation rates for water-permeable pavements. Water Science & Technology, 62 (5), 1161–1169.

STP, 1993. Standard tests procedure manual-asphalt mixes: retained Marshall stability. Saskatoon: Saskatchewhan Highways and Transportation.

Suresha, S.N., George, V. and Shankar, A.U.R., 2009. Evaluation of properties of porous friction course mixes for different gyration levels. Journal of Materials in Civil Engineering, 21 (12), 789–796.

Suresha, S.N., George, V. and Ravi Shankar, A.U.R., 2010. Effect of aggregate gradations on properties of porous friction course mixes. Materials and Structures, 43, 789–801.

Tan, S.A., Fwa, T.F. and Guwe, V.Y.K., 2000. Laboratory measurements and analysis of clogging mechanism of porous asphalt mixes. Journal of Testing and Evaluation, 28 (3), 207–216.

Tan, S.A., Fwa, T.F. and Chai, K.C., 2004. Drainage considerations for porous asphalt surface course design. Transportation Research Record: Journal of the Transportation Research Board, 1868, 142–149.

Tayfur, S., Ozen, H. and Aksoy, A., 2007. Investigation of rutting performance of asphalt mixtures containing polymer modifiers. Construction and Building Materials, 21 (2), 328–337.

TNZ, 2007. Specification for open graded porous asphalt. SP/SP 11 070704. Ararau Aotearoa: Transit New Zealand [TNZ].

Vavrik, W.R., et al., 2002. Bailey method for gradation selection in HMA mixture design. Transportation Research Circular E-C044, Washington, DC: National Research Council.

Watson, D.E., Masad, E., Moore, K.A., Williams, K. and Cooley, L.A. Jr., 2004. Verification of voids in coarse aggregate testing: determining stone-on-stone contact of hot-mix asphalt mixtures. Transportation Research Record: Journal of the Transportation Research Board, 1891, 182–190.

Zhu, Z.H., 2005. The application of ‘bailey method’ in porous asphalt (in Chinese). Unpublished master thesis. Taiwan National Cheng Kung University.

Table 1. Bulk specific gravity and water absorption of granite (Chen and Wong, 2016)

size range (mm)	bulk specific gravity	water absorption (%)
19.0-13.2	2.60 (± 0.007)*	
13.2-9.5	2.62 (± 0.002)	
9.5-6.3	2.58 (± 0.004)	0.48 (± 0.04)
6.3-4.75	2.60 (± 0.008)	
4.75-2.36	2.62 (± 0.010)	
< 2.36	2.60 (± 0.027)	1.29 (± 0.008)

Note: Value in parenthesis refers to standard deviation, and similarly elsewhere

Table 2. Mechanical properties of granite

property	value	specification requirement (LTA 2010)
L.A. abrasion value (%)	37.2	< 40
aggregate impact value (%, by mass)	27.9	< 30
10% fines value (kN)	179	> 130

Table 3. Properties of PG76 asphalt

property	result
relative density @ 25/25 °C	> 1.00
penetration @ 25 °C (0.1 mm)	> 50
softening point (°C)	> 80
loss on heating (% wt)	< 1.0
flash point (Cleveland cup) (°C)	> 230
toughness @ 25 °C (Nm)	>20
tenacity @ 25 °C (Nm)	> 15
mixing temperature (°C)	165-175
compaction temperature (°C)	155-165
viscosity @ 135 °C (Pa·s)	1.377
G*/sinδ at 76 ^{0} C, 10 rad/s (after RTFO, kPa)	2.648
G*/sinδ at 82 ^{0} C, 10 rad/s (after RTFO, kPa)	1.810
bending beam creep stiffness at -12 ^{0} C (MPa)	221
bending beam m-value* at -12 ^{0} C	0.31

Note: m-value= slope of the master stiffness curve at 60 seconds in bending beam rheometer (BBR) test

Table 4. Preliminary PAM gradation designs (Chen and Wong, 2016)

G	passing percentage by mass (%), on each sieve (mm)											ABC (%)
	19.0	13.2	9.5	6.3	4.75	2.36	1.18	0.6	0.3	0.15	0.075	
G1	100	80	74	50	14	5	5	5	5	5	5	3.3
G2	100	90	54	30	20	5	5	5	5	5	5	3.4
G3	100	85	70	60	30	10	9	8	7	6	5	3.8
G4	100	95	59	50	42	10	9	8	7	6	5	3.9
G5	100	90	66	30	21	15	13	11	9	7	5	4.2
G6	100	80	72	40	35	15	13	11	9	7	5	4.3
G7	100	95	51	40	24	20	17	14	11	8	5	4.7
G8	100	85	75	60	44	20	17	14	11	8	5	4.8

Table 5. Aggregate gradation designs for four newly-designed PAMs

G	passing percentage by mass (%), on each sieve (mm)										
	19	13.2	9.5	6.3	4.75	2.36	1.18	0.6	0.3	0.15	0.075
G_cont	100	77	59	40	30	7	6.6	6.2	5.8	5.4	5
G_coarse	100	70	45	20	12	7	6.6	6.2	5.8	5.4	5
G_fine	100	90	80	60	45	7	6.6	6.2	5.8	5.4	5
G_S	100	85	70	58	18	7	6.6	6.2	5.8	5.4	5

Table 6. Input parameters for ITSM test

parameter	values
test temperature (^{0} c)	25 ± 0.5
loading waveshape	haversine
loading pulse width (ms)	100
pulse repetition period, 10% to 90% (ms)	3000 ± 5seconds
target peak strain (με)	50 ± 20

Table 7. Results of air voids content and permeability

	TAV (%)	WAAV (%)	WAAV ratio (%)	$k \times 10^{-3}$ (cm/s)
G_cont	21.6 (± 0.6)	15.8 (± 0.7)	72.9 (± 2.2)	107.4 (± 10.6)
G_coarse	23.7 (± 0.8)	19.2 (± 1.1)	80.9 (± 3.1)	155.8 (± 13.0)
G_fine	22.3 (± 0.7)	15.9 (± 1.1)	71.0 (± 3.3)	126.4 (± 11.7)
G_S	23.6 (± 0.9)	17.7 (± 1.1)	75.1 (± 3.4)	160.9 (± 11.2)

Table 8. Results of Marshall test

	UC-MS (kN)	MC-MS (kN)	retained MS (%)
G_cont	6.5 (± 0.9)	6.1 (± 0.5)	93.5
G_coarse	6.0 (± 1.3)	5.9 (± 0.5)	98.1
G_fine	6.3 (± 0.9)	5.9 (± 0.4)	92.8
G_S	6.0 (± 0.7)	5.1 (± 0.3)	83.8

Table 9. Results of ITSM test

	UC-ITSM (MPa)	MC-ITSM (MPa)	retained ITSM (%)
G_cont	1899.5 (± 194.7)	1631.2 (±170.8)	85.9 (± 0.8)
G_coarse	1669.4 (± 76.1)	1427.5 (± 74.2)	85.6 (± 4.9)
G_fine	1560.3 (± 123.7)	1146.8 (± 160.6)	73.2 (± 4.6)
G_S	2373.8 (± 321.9)	1558.3 (± 118.3)	66.3 (± 6.1)

Table 10. Results of retained permeability

	CM	condition-ing	retained k (%)		$k \times 10^{-3}$ (cm/s)
			after conditioning	after five cycles	after five cycles
G_cont	CM1	no	/	13.8	14.4
	CM2	no	/	60.4	68.0
	CM1	ageing	93.1	15.9	17.1
	CM1	moisture	76.4	13.7	16.2
G_coarse	CM1	no	/	41.8	63.1
	CM2	no	/	89.5	136.7
	CM1	ageing	94.3	50.8	82.2
	CM1	moisture	86.1	41.7	65.2
G_fine	CM1	no	/	39.6	51.5
	CM2	no	/	79.0	93.9
	CM1	ageing	99.5	31.9	45.5
	CM1	moisture	92.1	31.7	42.2
G_S	CM1	no	/	31.5	50.9
	CM2	no	/	81.4	132.1
	CM1	ageing	98.1	40.6	64.8
	CM1	moisture	75.8	27.6	44.1

Figure captions

Figure 1

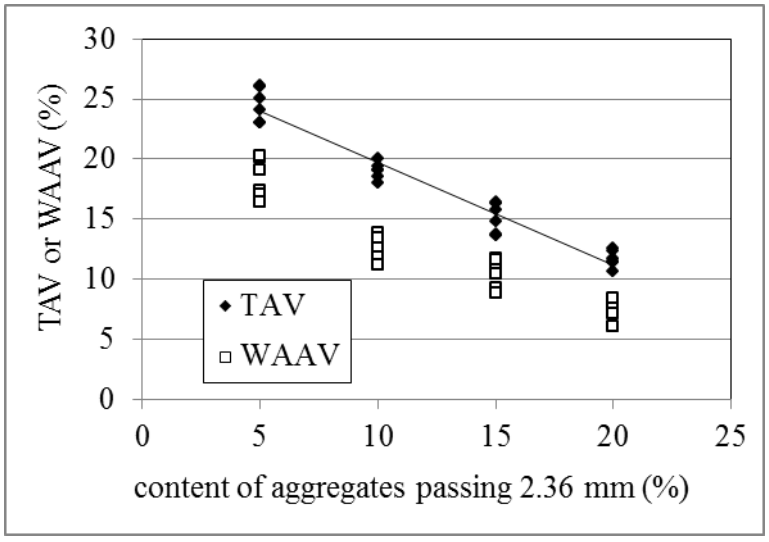
30
25
20
15
10
5
0
TAV or WAAV (%)
TAV
WAAV
0
5
10
15
20
25
content of aggregates passing 2.36 mm (%)

Figure 2

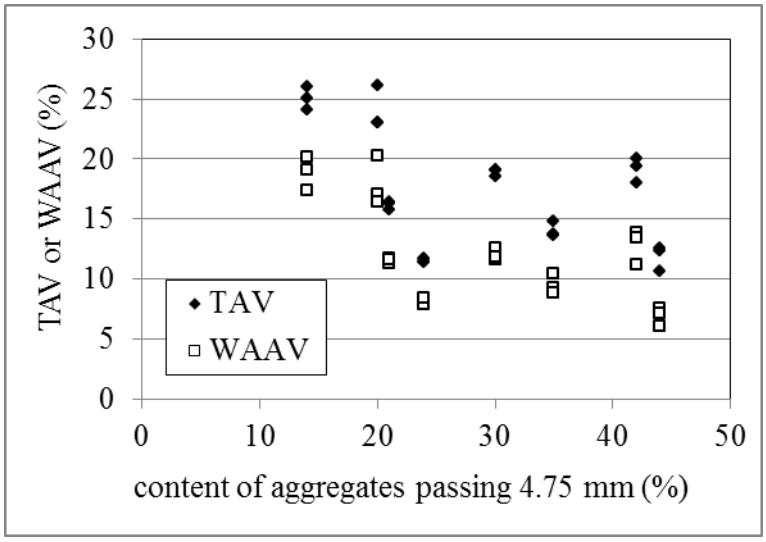
30
25
20
15
10
5
0
TAV or WAAV (%)
TAV
WAAV
0
10
20
30
40
50
content of aggregates passing 4.75 mm (%)

Figure 3

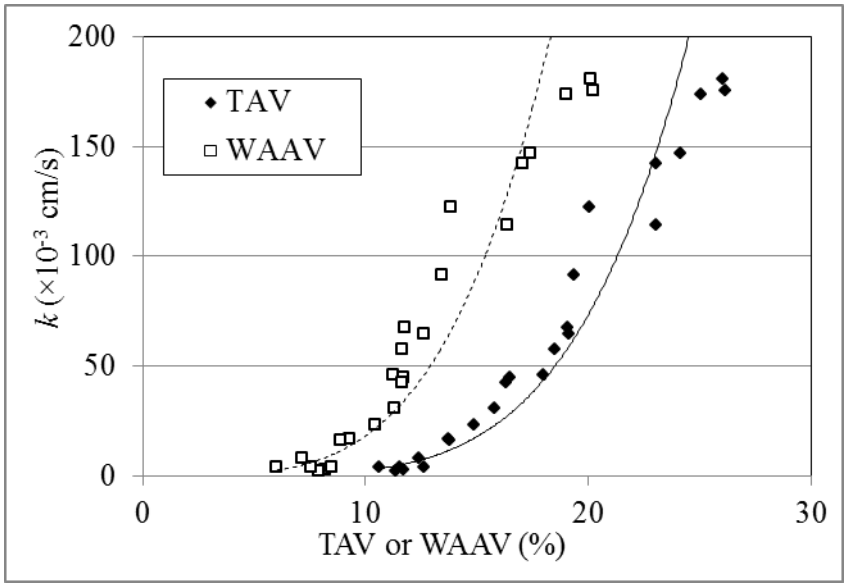

Figure 4

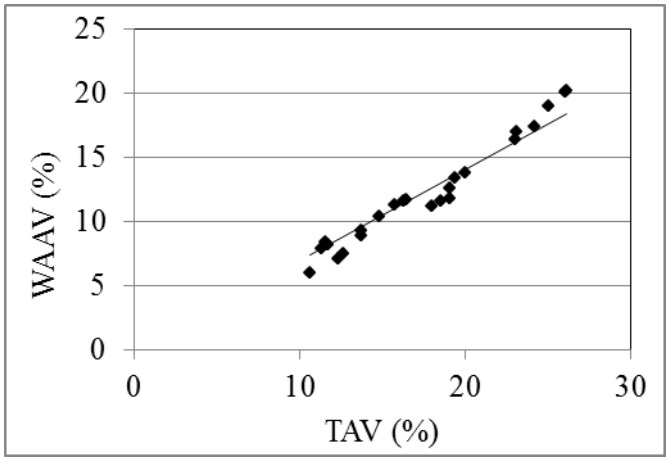

Figure 5

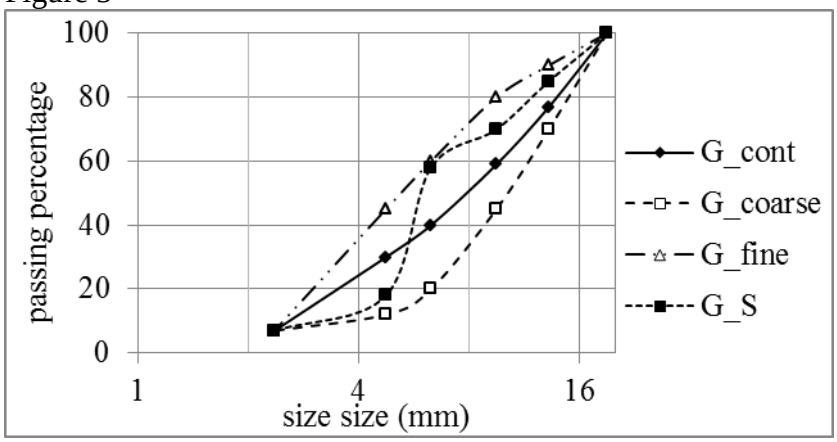
100
80
60
40
20
0
passing percentage
1
4
16
size size (mm)
G_cont
G_coarse
G_fine
G_S

Figure 6

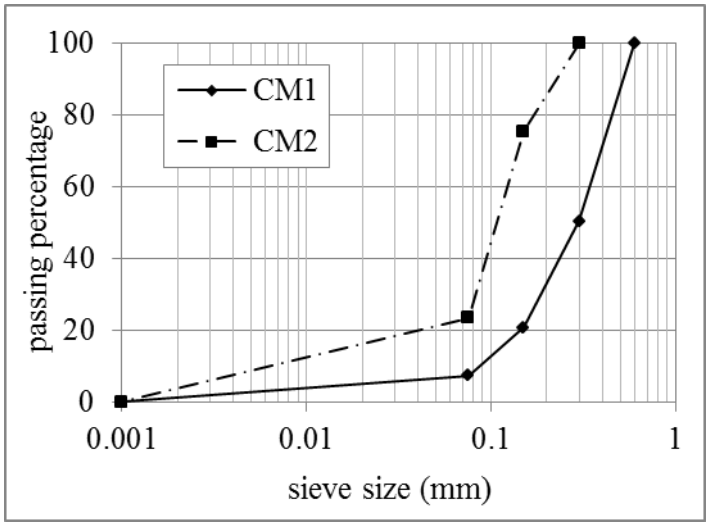
100
80
60
40
20
0
passing percentage
CM1
CM2
0.001
0.01
0.1
1
sieve size (mm)

Figure 7

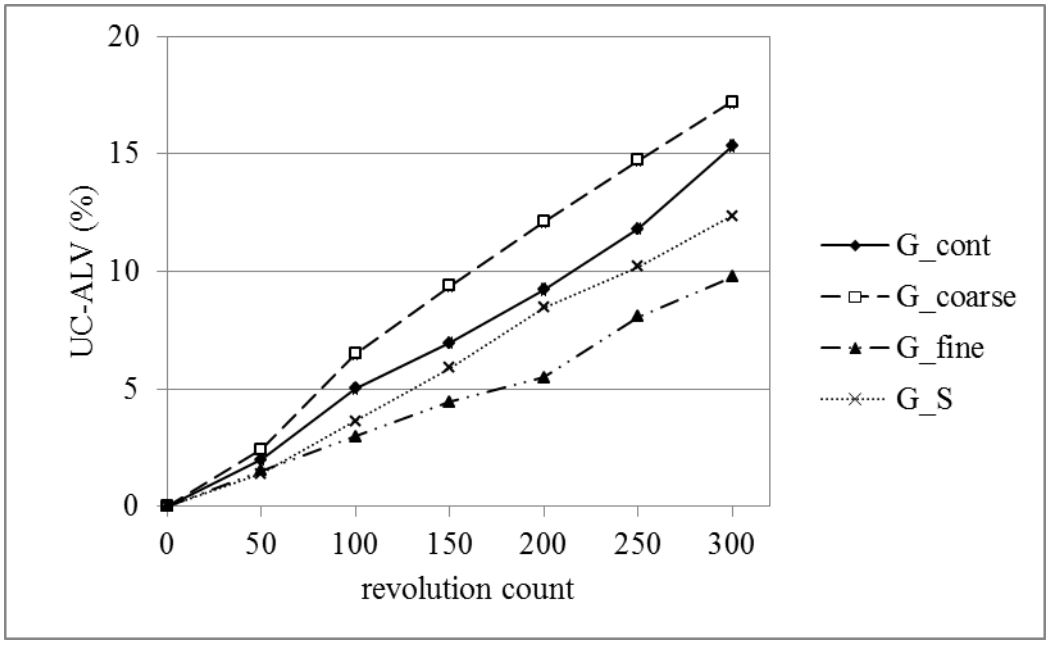
20
15
10
5
0
UC-ALV (%)
0
50
100
150
200
250
300
revolution count
G_cont
G_coarse
G_fine
G_S

Figure 8

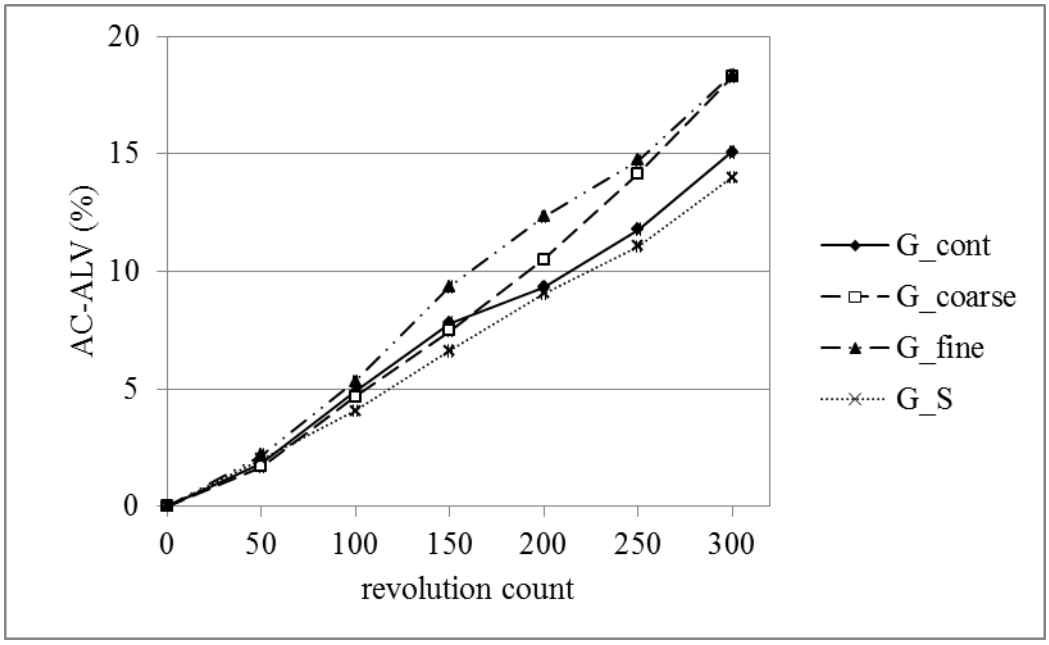
20
15
10
5
0
AC-ALV (%)
0
50
100
150
200
250
300
revolution count
G_cont
G_coarse
G_fine
G_S

Figure 9

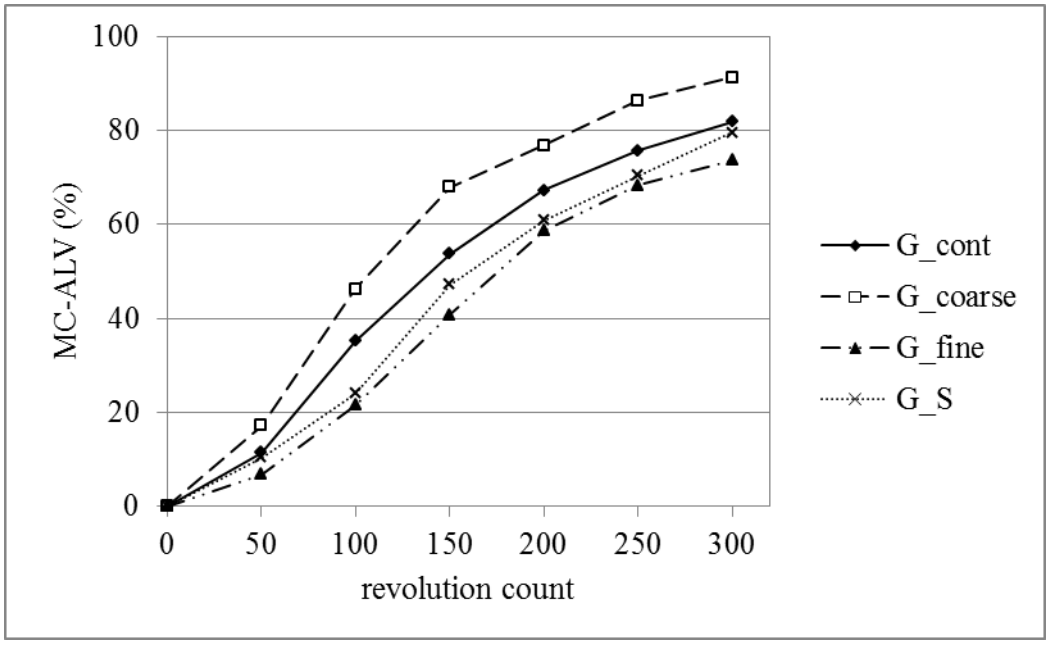
100
80
60
40
20
0
MC-ALV (%)
0
50
100
150
200
250
300
revolution count
G_cont
G_coarse
G_fine
G_S

Figure 10

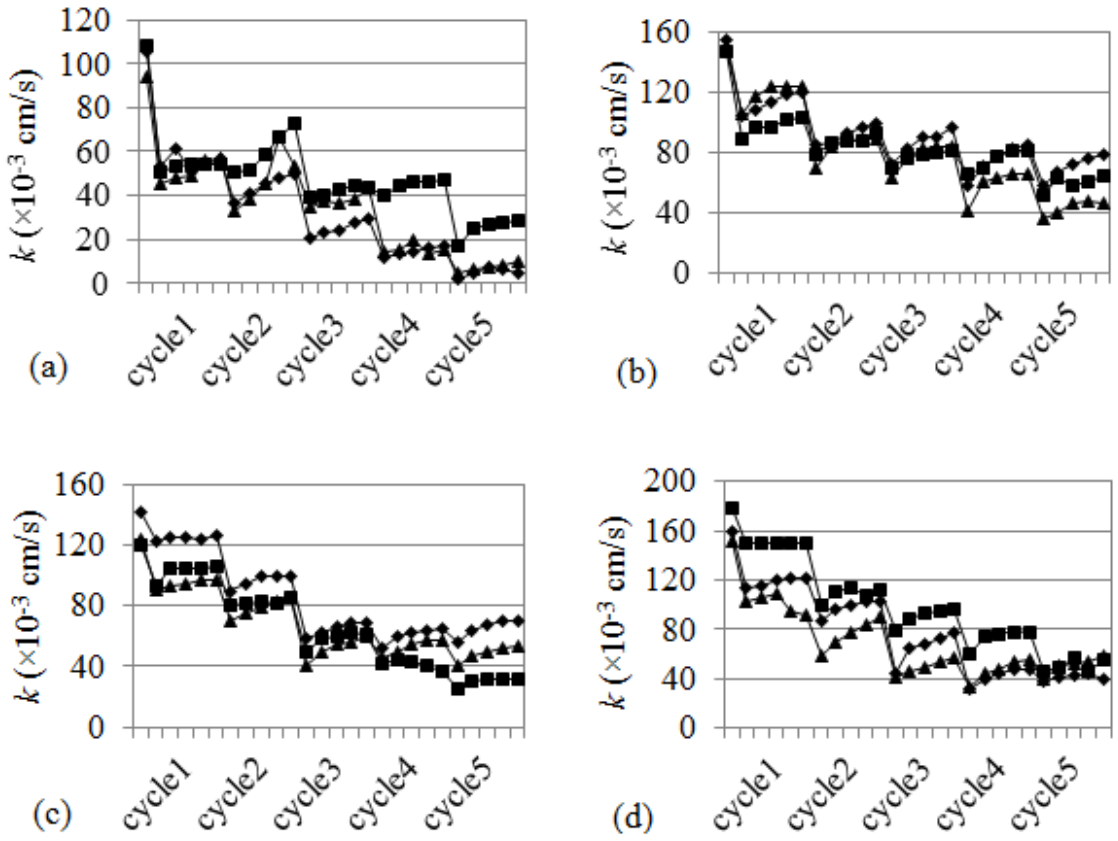
120
100
80
60
40
20
0
k (×10-3 cm/s)
cycle1
cycle2
cycle3
cycle4
cycle5
(a)
160
120
80
40
0
k (×10-3 cm/s)
cycle1
cycle2
cycle3
cycle4
cycle5
(b)
160
120
80
40
0
k (×10-3 cm/s)
cycle1
cycle2
cycle3
cycle4
cycle5
(c)
200
160
120
80
40
0
k (×10-3 cm/s)
cycle1
cycle2
cycle3
cycle4
cycle5
(d)

Figure 11

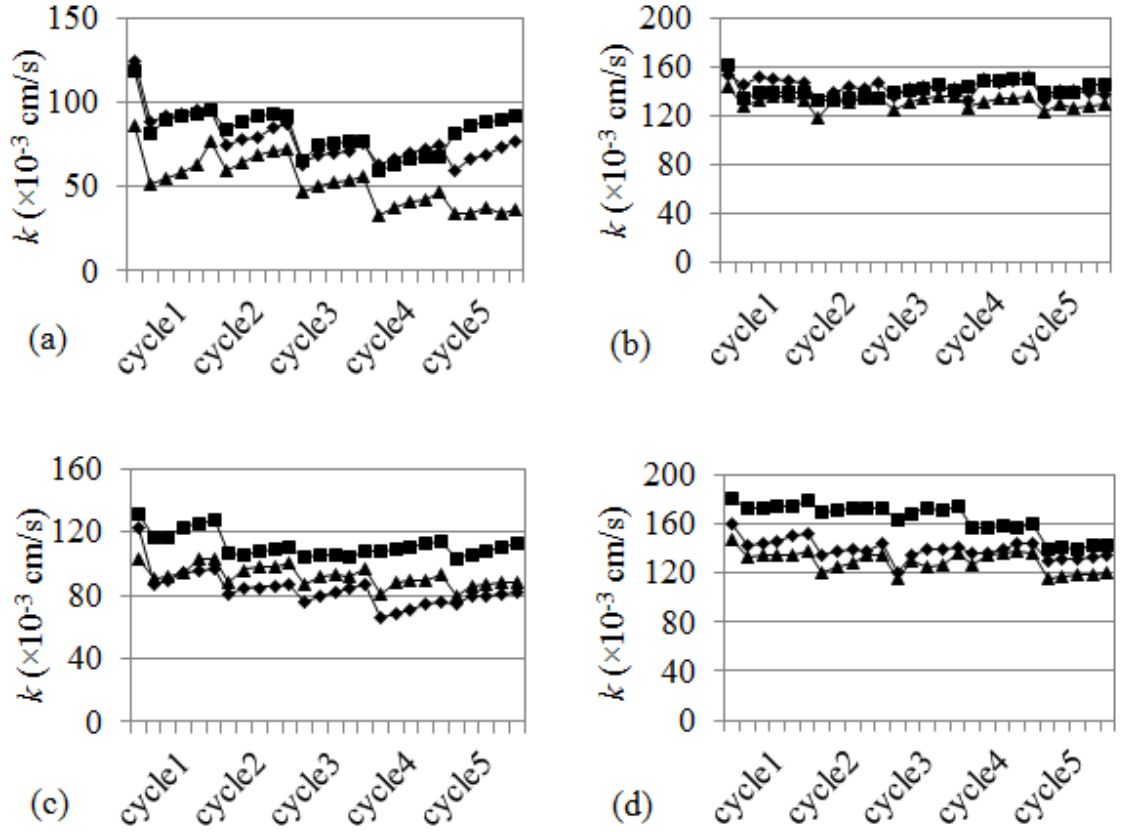
150
100
50
0
k (×10-3 cm/s)
(a)
cycle1
cycle2
cycle3
cycle4
cycle5
200
160
120
80
40
0
k (×10-3 cm/s)
(b)
cycle1
cycle2
cycle3
cycle4
cycle5
160
120
80
40
0
k (×10-3 cm/s)
(c)
cycle1
cycle2
cycle3
cycle4
cycle5
200
160
120
80
40
0
k (×10-3 cm/s)
(d)
cycle1
cycle2
cycle3
cycle4
cycle5